

The WiggleZ Dark Energy Survey: probing the epoch of radiation domination using large-scale structure

Gregory B. Poole,^{1,2*} Chris Blake,¹ David Parkinson,³ Sarah Brough,⁴
 Matthew Colless,⁴ Carlos Contreras,¹ Warrick Couch,¹ Darren J. Croton,¹
 Scott Croom,⁵ Tamara Davis,³ Michael J. Drinkwater,³ Karl Forster,⁶ David Gilbank,⁷
 Mike Gladders,⁸ Karl Glazebrook,¹ Ben Jelliffe,⁵ Russell J. Jurek,⁹ I-hui Li,¹⁰
 Barry Madore,¹¹ D. Christopher Martin,⁶ Kevin Pimbblet,¹² Michael Pracy,^{1,13}
 Rob Sharp,^{4,13} Emily Wisnioski,^{1,14} David Woods,¹⁵
 Ted K. Wyder⁶ and H. K. C. Yee¹⁰

¹Centre for Astrophysics & Supercomputing, Swinburne University of Technology, PO Box 218, Hawthorn, VIC 3122, Australia

²School of Physics, University of Melbourne, Parkville, VIC 3010, Australia

³School of Mathematics and Physics, University of Queensland, Brisbane, QLD 4072, Australia

⁴Australian Astronomical Observatory, PO Box 915, North Ryde, NSW 1670, Australia

⁵Sydney Institute for Astronomy, School of Physics, University of Sydney, NSW 2006, Australia

⁶California Institute of Technology, MC 278-17, 1200 East California Boulevard, Pasadena, CA 91125, USA

⁷South African Astronomical Observatory, PO Box 9, 7935 Observatory, Cape Town, South Africa

⁸Department of Astronomy and Astrophysics, University of Chicago, 5640 South Ellis Avenue, Chicago, IL 60637, USA

⁹Australia Telescope National Facility, CSIRO, Epping, NSW 1710, Australia

¹⁰Department of Astronomy and Astrophysics, University of Toronto, 50 St. George Street, Toronto, ON M5S 3H4, Canada

¹¹Observatories of the Carnegie Institute of Washington, 813 Santa Barbara Street, Pasadena, CA 91101, USA

¹²School of Physics, Monash University, Clayton, VIC 3800, Australia

¹³Research School of Astronomy & Astrophysics, Australian National University, Weston Creek, ACT 2600, Australia

¹⁴Max-Planck-Institut für extraterrestrische Physik, Giessenbachstraße, D-85748 Garching, Germany

¹⁵Department of Physics & Astronomy, University of British Columbia, 6224 Agricultural Road, Vancouver, BC V6T 1Z1, Canada

Accepted 2012 November 16. Received 2012 November 16; in original form 2012 August 31

ABSTRACT

We place the most robust constraint to date on the scale of the turnover in the cosmological matter power spectrum using data from the WiggleZ Dark Energy Survey. We find this feature to lie at a scale of $k_0 = 0.0160^{+0.0035}_{-0.0041}$ ($h \text{ Mpc}^{-1}$) (68 per cent confidence) for an effective redshift of $z_{\text{eff}} = 0.62$ and obtain from this the first ever turnover-derived distance and cosmology constraints: a measure of the cosmic distance–redshift relation in units of the horizon scale at the redshift of radiation–matter equality (r_H) of $D_V(z_{\text{eff}} = 0.62)/r_H = 18.3^{+6.3}_{-3.3}$ and, assuming a prior on the number of extra relativistic degrees of freedom $N_{\text{eff}} = 3$, constraints on the cosmological matter density parameter $\Omega_M h^2 = 0.136^{+0.026}_{-0.052}$ and on the redshift of matter–radiation equality $z_{\text{eq}} = 3274^{+631}_{-1260}$. We stress that these results are obtained within the theoretical framework of Gaussian primordial fluctuations and linear large-scale bias. With this caveat, all results are in excellent agreement with the predictions of standard Λ CDM models. Our constraints on the logarithmic slope of the power spectrum on scales larger than the turnover are bounded in the lower limit with values only as low as -1 allowed, with the prediction of $P(k) \propto k$ from standard Λ CDM models easily accommodated by our results. Finally, we generate forecasts to estimate the achievable precision of future surveys at constraining k_0 , $\Omega_M h^2$, z_{eq} and N_{eff} . We find that the Baryon Oscillation Spectroscopic Survey should substantially improve upon the WiggleZ turnover constraint, reaching a precision

* E-mail: gpoole@unimelb.edu.au

on k_0 of ± 9 per cent (68 per cent confidence), translating to precisions on $\Omega_M h^2$ and z_{eq} of ± 10 per cent (assuming a prior $N_{\text{eff}} = 3$) and on N_{eff} of $^{+78}_{-56}$ per cent (assuming a prior $\Omega_M h^2 = 0.135$). This represents sufficient precision to sharpen the constraints on N_{eff} from *WMAP*, particularly in its upper limit. For *Euclid*, we find corresponding attainable precisions on $(k_0, \Omega_M h^2, N_{\text{eff}})$ of $(3, 4, ^{+17}_{-21})$ per cent. This represents a precision approaching our forecasts for the *Planck Surveyor*.

Key words: surveys – cosmological parameters – large-scale structure of Universe.

1 INTRODUCTION

Recent decades have witnessed an incredible refinement of our cosmological model with significant advancements in the volume and redshift coverage of galaxy surveys, and in the methods of their analysis, playing a pivotal role. Such advances have opened up entirely new avenues of investigation, notably the use of features in the distribution of galaxies as standard rulers for direct geometric mapping of the Universe's expansion history.

The most investigated of these features are those induced by ‘baryon acoustic oscillations’ (BAOs) in the early-Universe’s photon–baryon fluid. The precise measurement across cosmic time of the BAO scale in the distribution of galaxies – a weak harmonic ripple with a comoving fundamental scale of ~ 105 ($\text{Mpc } h^{-1}$) – has been a major driver of recent and future galaxy redshift surveys and has received a great deal of attention in the recent literature (e.g. Cole et al. 2005; Eisenstein et al. 2005; Beutler et al. 2011; Blake et al. 2011a,c; Anderson et al. 2012).

Far less studied the ‘turnover’ in the galaxy power spectrum also represents a standard ruler in the observed distribution of galaxies. This feature, which is predicted to manifest on comoving scales of ~ 400 ($\text{Mpc } h^{-1}$) [or corresponding wavenumber $k_0 \sim 0.016$ ($h \text{ Mpc}^{-1}$)], was established at the epoch when the dynamics of the Universe transitioned from being dominated by relativistic material (photons and neutrinos) to being dominated by matter (dark and baryonic). This transition occurred because the mass-energy density of relativistic and non-relativistic materials declines differently with a , the expansion factor of the Universe. The particle density of both declines as $\rho \propto a^{-3}$; the per-particle energy of relativistic material also decreases with a due to redshift effects.

Previous to this transition from radiation domination to matter domination (at redshift z_{eq}), oscillations smaller than the horizon in the strongly coupled matter–radiation field were suppressed by the effects of radiation pressure while causally disconnected fluctuations larger than the horizon collapsed unhindered (see Eisenstein & Hu 1998). As a result, the scale-free primordial matter power spectrum believed to have emerged from inflation, $P(k) \propto k^{n_s}$ with $n_s \sim 1$, became distorted such that $P(k)$ became a decreasing function of k at small scales with a limiting behaviour $P(k) \propto k^{-3}$. At the turnover scale, a peak in $P(k)$ arose separating scales where $P(k)$ increased with k from those which decreased with k .

While the size of the horizon grew during the epoch of radiation domination, the scale of the turnover shifted ever larger to smaller values of k_0 until the epoch of matter domination commenced at redshift z_{eq} and the suppression of small-scale fluctuations ceased. From this point forward, all scales grew independently and by the same fractional amount while in the linear regime, and the comoving scale of the turnover became fixed. The exact size of this scale and the time of matter–radiation equality were influenced by the matter and radiation mass-energy den-

ties, $\Omega_M h^2$ and $\Omega_r h^2$, the latter being set by the effective number of extra relativistic degrees of freedom (N_{eff}) and by the photon mass-energy density ($\Omega_\gamma h^2$) which is well determined from observations of the temperature of the cosmic microwave background (CMB).

Analyses of the CMB have placed the most powerful constraints to date on parameters describing the epoch of matter–radiation equality by measuring z_{eq} , one of the ‘fundamental observables’ of the CMB (Komatsu et al. 2009). This measurement is made possible because of early integrated Sachs–Wolfe effects which manifest in the ratio of power between the first and third peaks in the angular power spectrum. The latest *WMAP* results find $z_{\text{eq}} = 3145^{+140}_{-139}$ (Komatsu et al. 2011).

Studies of the matter power spectrum on scales of the turnover can provide an additional window into physical processes operating at (or even prior to) the epoch of matter–radiation equality, a time before even the epoch of recombination observed by CMB experiments. While the precision of the turnover scale as a standard ruler is reduced by the fact that it was less sharply defined (fractionally speaking) than the BAO scale, its study benefits from lying firmly in the linear regime at all redshifts, easing complications which arise from non-linear structure formation and redshift-space distortions. As a result, structure on scales of the turnover are sensitive to non-Gaussian processes during inflation, permitting interesting new studies of early-Universe physics (Feldman, Kaiser & Peacock 1994; Durrer et al. 2003). For instance, scale-dependent bias effects are expected for galaxy samples with biases deviating from unity (e.g. Dalal et al. 2008), providing a rare opportunity to study inflation. Even in the case of Gaussian fluctuations, informative scale-dependent effects may be present on scales beyond the turnover (Yoo 2010).

The sensitivity of turnover scales to N_{eff} is also of interest, given the conflict of several recent CMB studies with conventional theoretical expectations. For the standard Λ CDM model, the expected value is $N_{\text{eff}} \sim 3.046$ (Mangano et al. 2005, i.e. slightly larger than 3 owing to the fact that neutrino decoupling was not instantaneous). However, recent high spatial resolution CMB measurements from the ACT and SPT observatories (Dunkley et al. 2011; Keisler et al. 2011) suggest a significantly higher result of $N_{\text{eff}} \sim 4$ (Hou et al. 2011; Calabrese et al. 2012; Smith, Das & Zahn 2012) leading several researchers to explore a class of ‘dark radiation’ models (e.g. Archidiacono, Calabrese & Melchiorri 2011).

The primary challenge to studies of the turnover, and the reason for its scant study to date, is the large volumes one must uniformly probe to detect it with any precision. While the fluctuations involved may lie on ~ 400 ($\text{Mpc } h^{-1}$) scales, many modes on these scales must be enclosed by a survey’s volume to permit a statistically significant analysis. Furthermore, subtle errors in the calibration of a survey’s selection function across its volume can easily lead to significant systematic power spectrum distortions on the survey’s

largest scales. This can be particularly serious for angular (i.e. 2D rather than 3D) measurements in imaging surveys which are much more sensitive to angular systematics in photometry and/or target selection (e.g. Ross et al. 2011, 2012).

Despite these challenges, several attempts have been made to measure the turnover or to study the matter power spectrum on its scales. The earliest attempts were performed using the APM galaxy survey (Baugh & Efstathiou 1993, 1994) or through studies of the distribution of optically selected galaxy clusters (Peacock & West 1992; Einasto, Gramann, Saar & Tago 1993; Scaramella 1993; Tadros, Efstathiou & Dalton 1998; Einasto et al. 1999). These studies have tended to observe turnovers at scales of $\sim 100\text{--}200$ ($\text{Mpc } h^{-1}$), which is quite discrepant with a wide range of modern cosmological probes and analyses. In all cases, either systematic effects induced by survey selection were found to dominate on turnover scales or rigorous studies of such issues were not performed. More recently, observations of quasars (Outram et al. 2003) and luminous red galaxies (LRGs) in the Sloan Digital Sky Survey (SDSS; York et al. 2000; Padmanabhan et al. 2007) have managed to measure power on scales reaching to those of the turnover, but relatively little analysis using this information has been performed.

In this paper, we present the most robust measurement of the turnover scale to date using data from the WiggleZ Dark Energy Survey (Drinkwater et al. 2010). WiggleZ is a large-scale galaxy redshift survey conducted with the AAOmega multi-object spectrograph on the Anglo-Australian Telescope at the Siding Spring Observatory. WiggleZ was designed to study the effect of dark energy on the Universe's expansion history and on the growth of cosmological structures across an unprecedented period of cosmic history. The primary science drivers for the survey have been the measurement of the BAO scale (e.g. Blake et al. 2011c), the growth of cosmological structure (e.g. Blake et al. 2011b) and the neutrino mass (e.g. Riemer-Sørensen et al. 2012) using the clustering pattern of ultraviolet-selected galaxies, as well as studies of the Universe's most actively star forming galaxies out to a redshift of 1.2 (Wisnioski et al. 2011; Li et al. 2012).

In this work, we treat the dominant systematic uncertainty of our study coming from convolution effects of the survey selection function and the subsequent extraction of the turnover scale in a statistically rigorous way. We also generate forecasts for the ongoing and future surveys of the Baryon Oscillation Spectroscopic Survey (BOSS; Eisenstein et al. 2011) and *Euclid* (Laureijs et al. 2011).

Our analysis is presented purely within the theoretical framework of Gaussian primordial fluctuations. Models which permit non-Gaussian primordial fluctuations provide for a wide range of large-scale clustering behaviours and we will leave their exploration for future work.

In Section 2, we present our method of constructing a galaxy power spectrum from the WiggleZ data set which is optimized for studies of the turnover. In Section 3, we extract the turnover scale from the WiggleZ observations and present the resulting distance measurement to $z = 0.62$ and constraints on $\Omega_M h^2$ and z_{eq} . In Section 4, we generate forecasts for future surveys (highlighting results for BOSS and *Euclid*), estimating the volume dependence of turnover scale measurement precision and of resulting cosmology constraints. We also compute the constraints in the $N_{\text{eff}}\text{--}\Omega_M h^2$ plane from the CMB observations of *WMAP* and forecast the constraints achievable by the *Planck Surveyor*. Finally, we present some discussion and our conclusions in Section 5.

Our choice of fiducial cosmology throughout will be a standard ΛCDM model with $\Omega_M = 0.27$, $\Omega_\Lambda = 0.73$ and $h = 0.7$, unless otherwise stated.

2 OBSERVATIONS

In this section, we present our construction of the WiggleZ power spectrum for use in our turnover analysis. This will include our methods of deconvolving the effects of the survey selection function, of co-adding the power spectra observed in seven independent WiggleZ survey regions and our treatment of the survey's radial selection function, the dominant source of systematic uncertainty in this current analysis.

2.1 The WiggleZ power spectrum

To construct a power spectrum for this study, we followed the general approach described by Blake et al. (2010, see section 3.1). To summarize, we used the optimal weighting scheme of Feldman et al. (1994, FKP), converting redshifts to distances using our fiducial ΛCDM cosmological model. We individually enclosed the survey cones of each region within cuboids of sides (L_x , L_y , L_z) and map each region's observed galaxy distribution on to a grid with dimensions (n_x , n_y , n_z) using the 'nearest grid point' assignment scheme. Denoting the resulting distribution as $n(\mathbf{x})$, we then applied a fast Fourier transform to the resulting grid, weighted in accordance with the method described in FKP [as given by equation 9 of Blake et al. 2010, using a weighting factor more appropriate for our turnover analysis of $P_0 = 20\,000$ ($\text{Mpc } h^{-1}$) 3], to produce $n(\mathbf{k})$. The corresponding values for each WiggleZ region are presented in Table 1. In the later sections, we will require the covariance between the bins in our WiggleZ $P(k)$. This was also determined following the procedure of FKP as presented in section 3.1 (equation 20) of Blake et al. (2010). We note that increasing the characteristic amplitude used in the FKP weighting from $P_0 = 2500$ ($\text{Mpc } h^{-1}$) 3 used previously for WiggleZ BAO studies could amplify systematics originating from low-density regions, but in practice we find the consequences are not significant for this data set.

Both the FKP weighting and the conversion of $n(\mathbf{k})$ to our final estimate of the power spectrum, $P(k)$, depend critically on the survey selection function, $W(\mathbf{x})$. This function expresses the expected mean density of galaxies with spectroscopic redshifts at position \mathbf{x} , given the angular and luminosity survey selection criteria. Again, we follow the procedure of Blake et al. (2010, see section 2) to determine the angular and radial contributions to $W(\mathbf{x})$. While angular effects are estimated in precisely the same manner as described in Blake et al. (2010) – accounting for effects such as the coverage mask, spatial variations in dust extinction and radial completeness of each individual 2dF pointing contributing to the survey – our estimation of radial contributions to the survey selection function required some modification which is described below in Section 2.1.3.

While aliasing from the assignment scheme only affects the power spectrum on scales far smaller than the turnover, we nevertheless correct for this effect using the method described by Jing (2005). Furthermore, since the survey target density is obtained from the survey itself, we correct for a potential large-scale $P(k)$ bias in a manner analogous to the integral constraint of correlation functions (see e.g. equation 25 of Peacock & Nicholson 1991) by applying a boost to the measured $P(k)$ near $k = 0$, generated using the Fourier transform of the window function.

Table 1. A summary of parameters relevant to our calculation of the WiggleZ galaxy power spectrum for each observed region. The values of (L_x , L_y , L_z) specify the dimensions of the cuboid used to enclose each region and (n_x , n_y , n_z) specify the corresponding grid dimensions of the cuboid. Volume and N_{gal} are the volume and number of galaxies contributing to our measurement in each region (spanning the redshift range $[z_{\min}, z_{\max}] = [0.4, 0.8]$), respectively, while n is the resulting average number density of galaxies in each region.

Region	L_x (Mpc h^{-1})	L_y (Mpc h^{-1})	L_z (Mpc h^{-1})	n_x	n_y	n_z	Volume (Gpc h^{-1}) ³	N_{gal}	n (Mpc h^{-1}) ⁻³
9-hour	899.4	520.7	315.5	256	128	64	0.148	18 978	1.28×10^{-4}
11-hour	899.5	520.7	318.9	256	128	64	0.149	20 170	1.35×10^{-4}
15-hour	907.7	694.7	353.4	256	128	64	0.223	30 015	1.35×10^{-4}
22-hour	894.4	335.1	338.6	256	64	64	0.101	16 146	1.59×10^{-4}
1-hour	891.8	300.7	252.4	256	64	64	0.0677	8304	1.23×10^{-4}
3-hour	893.1	313.3	305.6	256	64	64	0.0855	10 241	1.20×10^{-4}
0-hour	891.6	241.1	297.8	256	64	64	0.0640	7409	1.16×10^{-4}

Finally, to ensure a power spectrum optimized for studying scales around the turnover, we have made the following three adjustments to the procedure described in Blake et al. (2010).

2.1.1 Redshift range

The redshift range used in our analysis has two competing effects on our analysis. By increasing the range used we increase the effective volume of our measurement, increasing the number of modes probed by our study at scales of the turnover and increasing the signal of our volume-limited measurement. Unfortunately, doing so also leads to a less plane-parallel survey geometry, increasing the covariance induced by the survey selection function on our largest scale modes.

We have performed our analysis on several redshift ranges $[z_{\min}, z_{\max}]$, varying z_{\min} from 0.3 to 0.4 and z_{\max} from 0.8 to 0.9. While the choice over these ranges does not have a strong effect on our results, we have found the range $[0.4, 0.8]$ to yield slightly optimal results since it maintains minimal covariance between neighbouring $P(k)$ bins while providing a near maximally precise measurement. Hence, we will use this range throughout our analysis.

2.1.2 Choice of Fourier binning

We perform all our analysis on power spectra binned by wavenumber (k). Our choice of binning also introduces two competing effects. By increasing the size of our power spectrum bins, we increase the signal and reduce the covariance of neighbouring bins, increasing the precision of our power spectra. Unfortunately, we are trying to fit to a feature at small values of k and the use of bins that are too large will prevent us from resolving it. We have experimented with a variety of bin sizes ranging from $\delta k = 0.005$ (h Mpc $^{-1}$) to 0.02 (h Mpc $^{-1}$) and have found the use of $\delta k = 0.005$ (h Mpc $^{-1}$) to be optimal. We deemed further reduction of this binning unwarranted, given the low signal at this point for modes larger than the turnover in several regions. In all cases, the medians of the $|k|$ values contributing to each bin are used to represent their positions.

2.1.3 Radial selection function

At the mean of our chosen redshift range, the maximum scale probed by WiggleZ in directions transverse to the line of sight is ~ 500 (Mpc h^{-1}), while the comoving distance along the line of sight from $z_{\min} = 0.4$ to $z_{\max} = 0.8$ is ~ 900 (Mpc h^{-1}). As a result, most of the information in WiggleZ on scales of the turnover is contained within radial modes. Consequently, our estimate of the WiggleZ radial

selection function is a significant source of systematic uncertainty in our present analysis.

We have examined several approaches to determining the WiggleZ radial selection function based on the approach presented in Blake et al. (2010, see section 2.5). Summarizing briefly, we fit a smooth analytic function to the observed redshift distribution $N(z)$ for each observing priority band (WiggleZ observations were prioritized by magnitude, with apparently faint galaxies given highest priority and each band representing an equal interval of $20.0 \leq r \leq 22.5$). In this procedure, we must choose a functional form with which to parametrize the observed WiggleZ $N(z)$. In past efforts, this procedure has been performed on each of the seven WiggleZ survey regions *independently* using a polynomial of order dynamically chosen to be that above which the reduced χ^2 statistic does not decrease.

We have re-examined this procedure using several approaches three of which are presented here: the standard polynomial fit applied to each region independently [i.e. the standard approach of past work, denoted by the ‘polynomial $N(z)$ ’ method], a cubic spline similarly fitted to each region separately [denoted by the ‘spline $N(z)$ ’ method] and a polynomial fit to the total sum of $N(z)$ for all Northern Galactic Pole (NGP) fields jointly and all Southern Galactic Pole (SGP) fields jointly [denoted by the ‘joint polynomial $N(z)$ ’ method; note, due to differing optical selection, the WiggleZ NGP and SGP fields have differing radial selection functions]. The motivation of this last method is to reduce the effects of cosmic variance by combining regions but carries the risk of being susceptible to region-to-region systematics. The influence of this choice on our resulting WiggleZ $P(k)$ is shown in Fig. 1 where we show the deconvolved WiggleZ power spectrum for the whole survey sample (see Section 2.2 below for details). As noted in Blake et al. (2010), only results for $k < 0.03$ (h Mpc $^{-1}$) are significantly affected by the details of our radial selection estimation, leaving the scales of the BAO unaffected.

We have carried out our analysis through each of these methods and find relatively little effect on our turnover constraints and no qualitative change to the conclusions of this study. The challenge in the procedure of determining $N(z)$ for this purpose is to choose a functional form nuanced enough to capture the selection induced by the survey strategy and telescope operations but smooth enough not to fit (and hence remove) the real structure we seek to measure. Hence, for this reason, we favour the joint polynomial $N(z)$ and for all subsequent analyses we quote results derived using this approach.

Finally, our method includes a full k -dependent correction for misidentified redshifts (referred to as redshift ‘blunders’) using the survey simulations described in section 3.2 of Blake et al. (2010). This includes blunders both from constant multiple shifts due to

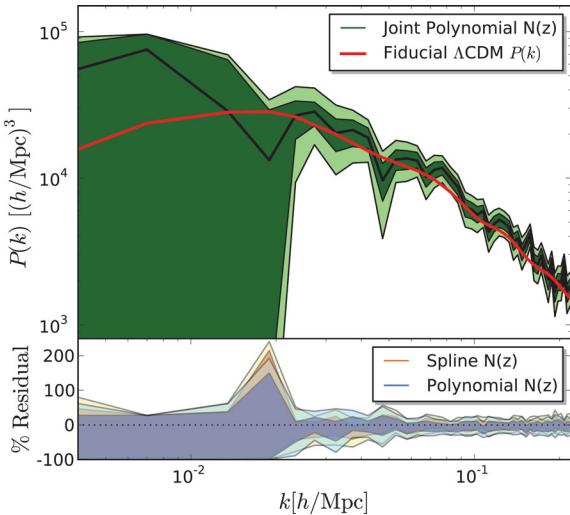


Figure 1. The deconvolved co-added WiggleZ $P(k)$ using three different methods for estimating the WiggleZ radial selection function (a cubic spline or a polynomial fit to each region independently and our preferred method: a polynomial fit jointly to the NGP and SGP fields). The dark shaded regions depict 68 per cent confidence intervals and the light-shaded regions depict 95 per cent confidence intervals. The solid black line depicts the maximum likelihood $P(k)$. The red line depicts a Λ CDM model incorporating a simple model for redshift-space distortions. Residuals (in the bottom panel) depict results after subtraction of the joint spline maximum likelihood $P(k)$, illustrating the magnitude of systematic effects associated with uncertainties in the WiggleZ radial selection function.

emission-line misidentifications and from a continuous range of misidentified sky lines into a lognormal simulation including the full selection function. The redshift blunder model is based on thousands of repeat redshifts obtained during the survey. We find this correction to be small compared to the $P(k)$ uncertainty for the scales relevant to our turnover analysis.

2.2 Deconvolution of the survey selection function

The WiggleZ survey was conducted within seven separate survey regions, each with different selection functions due to varying optical selection, region boundary geometries, observing conditions and dust attenuations. While much of our analysis in later sections will involve direct fits applied jointly to the data of these regions, we seek here to generate a single deconvolved power spectrum of the full survey sample, with the effects of differing selection functions removed, in order to present the data contained in the survey on its largest scales.

To achieve this, we use a Markov chain Monte Carlo (MCMC) approach. Using the Metropolis–Hastings algorithm, we generate random sets of propositions for the deconvolved power spectra we seek, convolve each set seven times using the window function of each region and compute the joint likelihood of these convolved proposition sets against the observed power spectrum of each region. We compute this likelihood using the full information of each region’s covariance matrix. We optimize this calculation by drawing propositions from a rotated covariance matrix constructed from a short secondary burn-in period following a primary burn-in designed to erase the memory of the starting point of our calculation. We use 10^5 iterations for each burn-in phase and 2×10^6 propositions for the final integration used to determine the posterior distribution of our 50 observed, deconvolved power spectrum bins. All

chains have been inspected to ensure that they are well mixed. To increase the efficiency of our calculation, we use the matrix multiplication approach presented in Blake et al. (2010, equation 17) to convolve our $P(k)$ proposition sets with each region’s selection function. We have verified that this approach remains equivalent to a full 3D convolution on all scales utilized for this current analysis.

The results of this calculation are presented in Fig. 1. In this figure, we see that at scales $k < 0.03$ ($Mpc h^{-1}$), the deconvolved co-added WiggleZ power spectrum places useful constraints on the maximum power permitted on scales at and beyond the turnover, but places little or no constraint on the minimum permitted power. For comparison, we also show (in red) a Λ CDM power spectrum in our fiducial cosmology with a simple model for redshift-space effects. This is obtained by taking a biased non-linear (Smith et al. 2003, i.e. halofit) power spectrum from the Boltzmann code CMB (Lewis, Challinor & Lasenby 2000) and applying the redshift-space distortion model of Kaiser (1987) with a Lorentzian damping term (see equation 9 of Blake et al. 2011b). The parameter values of the galaxy bias ($b^2 = 1.18$), redshift-space distortion parameter ($\beta = f/b = 0.69$) and the variable damping term ($\sigma_v = 300 \text{ km s}^{-1}$) needed for this model were obtained from fits to the 2D power spectrum obtained from the WiggleZ NGP fields. Fig. 1 illustrates that this model provides an excellent fit to the WiggleZ power spectrum over the full range of scales presented.

3 ANALYSIS

In this section, we will present our extraction of turnover information from the WiggleZ power spectrum presented in Section 2 as well as the distance and cosmology constraints obtainable from this measurement.

3.1 Measurement of the WiggleZ turnover scale

To extract information about the turnover from the observed WiggleZ power spectrum, we have followed the method of Blake & Bridle (2005). This approach is model-independent in the sense that it does not take cosmological parameters or model power spectra from Boltzmann codes as inputs. Specifically, we fit (using the same MCMC machinery and chain lengths as described in Section 2.2) the following model, convolved with the WiggleZ selection functions and jointly fitted to all seven WiggleZ regions:

$$\log_{10} P(k) = \begin{cases} \log_{10} P_0 (1 - \alpha x^2) & \text{if } k < k_0, \\ \log_{10} P_0 (1 - \beta x^2) & \text{if } k \geq k_0, \end{cases} \quad (1)$$

$$\text{where } x = \left(\frac{\ln k - \ln k_0}{\ln k_0} \right). \quad (2)$$

We marginalize over P_0 , since its interpretation is complicated by degenerate normalizing parameters such as σ_8 and the bias of WiggleZ galaxies, and over β since its interpretation is complicated by all the cosmological parameters, redshift-space and scale-dependent bias effects which influence the overall shape of $P(k)$ on scales smaller than the turnover. Hence, we focus here on just two parameters: k_0 and α , which carry information about the position of the peak in $P(k)$ and whether we have detected a drop in power at scales larger than this peak (this is the case if $\alpha > 0$). All cosmology constraints derived from our measurement of the turnover will be based purely on our measurement of k_0 . For our fiducial Λ CDM cosmology, the expected value is $k_0 = 0.016 (h \text{ Mpc}^{-1})$.

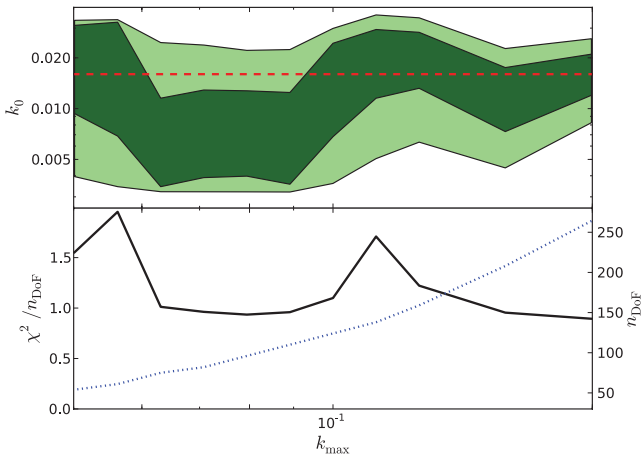


Figure 2. Results of fitting our logarithmic parabola turnover model (see equation 4) to the observed WiggleZ $P(k)$ as a function of the maximum range in k used for the fit (k_{\max}). Top panel: dark-shaded regions depict 68 per cent confidence intervals and light-shaded regions depict 95 per cent confidence intervals. The red dashed line depicts the theoretical expectation for a standard Λ CDM model. Bottom panel: the black line depicts the reduced- χ^2 statistic and the dotted blue line depicts the number of degrees of freedom (n_{DoF}). We see from this that our measured turnover scale is stable and yields an acceptable fit for $k_{\max} \gtrsim 0.1$.

Since the real power spectrum has a changing logarithmic slope with k at scales smaller than the turnover, we need to carefully consider the maximum of the range of scales over which we perform our fit (denoted by k_{\max}) to avoid systematic biases. We have performed our fit using a range of k_{\max} and present the results in Fig. 2. Here we see that the results of our fit for k_0 are both stable and acceptable (as measured by the reduced χ^2 statistic) for $k_{\max} \gtrsim 0.1$. However, non-linear effects which alter the logarithmic slope of the power spectrum are expected to become significant for $k > 0.2 (h \text{ Mpc}^{-1})$ and so we limit our fit with $k_{\max} = 0.2 (h \text{ Mpc}^{-1})$ for the remainder of our analysis.

The final marginalized results for k_0 from our fit are $k_0 = 0.0160^{+0.0035}_{-0.0041}$ (68 per cent confidence) and $0.0160^{+0.0073}_{-0.0075}$ (95 per cent confidence). Our results are not well constrained for α where we measure lower limits of $\alpha > -1.32$ (95 per cent) with a hard prior $\alpha < 10$. In Fig. 3 we present the 2D marginalized posterior distribution function (PDF) of our fit to the WiggleZ power spectrum in the $\alpha-k_0$ plane. We can see from this figure that our analysis constrains k_0 lie near the theoretical value of $k_0 \sim 0.016 (h \text{ Mpc}^{-1})$. Furthermore, α is constrained to $\alpha \gtrsim -1$ indicating that $P(k)$ is either an increasing function of k or nearly constant at scales larger than the turnover. The long tail to positive values of α reflects the lack of constraint WiggleZ places on the minimum power allowed on the largest scales of the survey.

Negative values of α are marginally allowed by our fit, permitting a power spectrum which does not formally exhibit a turnover. To aid our interpretation of this result, we have overlaid on to Fig. 3 (with white contours) a model which presents the logarithmic slope (denoted by n) for $P(k < k_0) \propto k^n$ implied by equation (1) between k_0 and our largest scale bin at $k = 0.005 (h \text{ Mpc}^{-1})$. This model incorporates the strong and tight degeneracy

$$\log_{10} P_0 = -0.67 \log_{10} k_0 + 3.12 \quad (3)$$

present in our fit. From this we can see that WiggleZ constrains the power at scales larger than the turnover to $n > -1$ at nearly 95 per cent confidence. The large- k asymptotic value of $n = -3$ is

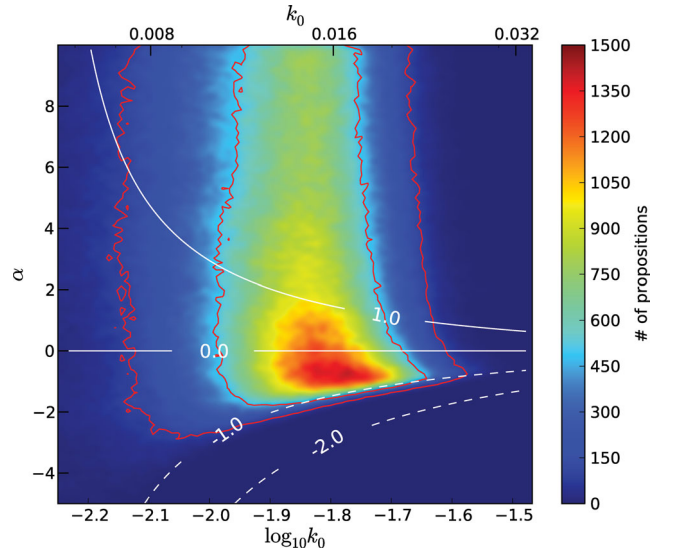


Figure 3. The 2D marginalized PDF in the $\alpha-k_0$ plane from fitting our logarithmic parabola turnover model (see equation 4) to the observed WiggleZ $P(k)$. The red contours depict the 68 and 95 per cent confidence regions. The white contours depict the loci of several values of n for the model $P(k \leq k_0) \propto k^n$. From this plot we see that the WiggleZ $P(k)$ has an inflection at $k_0 \sim 0.016 (h \text{ Mpc}^{-1})$ with $n > -1$, distinctly different from the asymptotic value for $P(k > k_0)$ of $n = -3$. Our fit easily accommodates the theoretical expectation of $k_0 = 0.016 (h \text{ Mpc}^{-1})$ and $n = 1$ for a standard Λ CDM model.

completely ruled out, meaning that we have certainly detected an inflection in the logarithmic slope of $P(k)$. With the theoretically expected value of $n = 1$ easily accommodated by our fit, and a preferred scale for the $P(k)$ inflection of $k_0 \sim 0.016 (h \text{ Mpc}^{-1})$, we thus find that our turnover fit is in good agreement with the theoretical expectations of a standard Λ CDM model.

3.2 The WiggleZ turnover distance measurement

The scale of the turnover roughly corresponds to the scale of the horizon at the epoch of matter–radiation equality (k_H) given by (see Prada et al. 2011)

$$k_H = (4 - 2\sqrt{2})r_H^{-1}, \quad (4)$$

$$\text{where } r_H = c \int_0^{(1+z_{\text{eq}})^{-1}} \frac{da}{a^2 H(a)} \quad (5)$$

with $H(a)$ being the Hubble expansion rate given by

$$H^2(a) = H_0^2 (\Omega_r a^{-4} + \Omega_M a^{-3} + \Omega_\Lambda), \quad (6)$$

where H_0 being the Hubble constant. This yields a horizon scale of $r_H = 117.9 (\text{Mpc})$ corresponding to $k_H = 0.014 (h \text{ Mpc}^{-1})$ for the WMAP result of $z_{\text{eq}} = 3145$ (Komatsu et al. 2011) in our fiducial Λ CDM cosmology. However, the actual precise position of the peak of $P(k)$ can differ significantly from this value. Indeed, using the Boltzmann code CMB (Lewis et al. 2000), we find that the turnover scale in our fiducial cosmology is $k_{0,\text{fid}} = 0.0159 (h \text{ Mpc}^{-1})$.

As discussed in Section 2.1.3, the largest scales of the power spectrum utilized in this work are dominated by radial modes. However, for most of the scales involved in our turnover fit, this is not the case. For this reason, we choose to convert our measurement of the turnover scale into a distance measurement following the approach introduced by Eisenstein et al. (2005) for BAO studies. Through

this approach, our turnover measurement constrains the dilation measure D_V defined as

$$D_V(z) = \left[(1+z)^2 D_A^2(z) \frac{cz}{H(z)} \right]^{1/3}, \quad (7)$$

where c is the speed of light, $D_A(z)$ is the angular diameter distance at redshift z and $H(z)$ is given by equation (6) with $a = (1+z)^{-1}$. We will obtain this quantity using the assumption that distances scale proportionally by the same ‘stretch factor’ ($\tilde{\alpha}$) under small perturbations from a fiducial cosmology. Given the turnover scale in our fiducial cosmology, we obtain this stretch factor from

$$\tilde{\alpha} = k_{\text{fid}}/k_0. \quad (8)$$

We will express this dilation measure in a dimensionless form using units of the $z = 3145$ horizon size (r_H) as $d_t = D_V/r_H$. We choose this scale instead of the turnover scale from `CAMB` to render the result less model-dependant.

For this method we require an effective redshift for our measurement, which we compute by determining the effective redshift at $k = 0.015 (h \text{ Mpc}^{-1})$ for the power spectrum used in this analysis. This is achieved using equation (13) of Blake et al. (2011c) from which we obtain $z_{\text{eff}} = 0.62$, quite similar to the effective redshift of other WiggleZ studies.

The dilation measure at z_{eff} in our fiducial cosmology is $d_{t,\text{fid}}(z_{\text{eff}} = 0.62) = 18.41$. For our measurement of $k_0 = 0.0160^{+0.0035}_{-0.0041}$ (68 per cent) and $0.0160^{+0.0073}_{-0.0075}$ (95 per cent), we obtain a stretch factor $\tilde{\alpha} = 0.99^{+0.34}_{-0.18}$ (68 per cent) and $0.99^{+0.88}_{-0.31}$ (95 per cent). Scaling with respect to our fiducial cosmology using this stretch factor, we thus obtain a model-independent distance of $d_t(z_{\text{eff}} = 0.62) = 18.3^{+6.3}_{-3.3}$ (68 per cent) and $18.3^{+16.1}_{-5.7}$ (95 per cent). Assuming the fiducial turnover scale given above, this corresponds to $D_V(z_{\text{eff}} = 0.62) = 2156^{+743}_{-387}$ (68 per cent) and 2156^{+1900}_{-676} (95 per cent) (Mpc).

3.3 Cosmology constraints from the WiggleZ turnover measurement

To calibrate the scale of the turnover as a function of cosmology, we ran `CAMB` to produce a series of matter power spectra, fixing all parameters to our fiducial cosmology but allowing $\Omega_M h^2$ to vary for several choices of N_{eff} . The results are presented in Fig. 5 where we illustrate our method of converting measurements of k_0 into cosmological constraints.

The position of the turnover depends on $\Omega_M h^2$ and N_{eff} in the following way (see Komatsu et al. 2009). First, through the dependence of the total energy density of relativistic material on N_{eff} given by

$$\Omega_r = \Omega_\gamma (1 + 0.2271 N_{\text{eff}}), \quad (9)$$

$$\text{where } \Omega_\gamma = \frac{8\pi G}{3H_0^2} \frac{4\sigma_B T_{\text{CMB}}^4}{c^3}, \quad (10)$$

with Ω_γ being the energy density of photons,¹ G being Newton’s gravitational constant, σ_B being the Stefan–Boltzmann constant, and T_{CMB} being the temperature of the CMB, and, secondly, through

¹ Note that due to the precision with which the CMB temperature is measured ($T_{\text{CMB}} = 2.72548 \pm 0.00057 \text{ K}$, Fixsen 2009), the photon energy density is precisely known to be $\Omega_\gamma h^2 = 2.47274 \times 10^{-5}$.

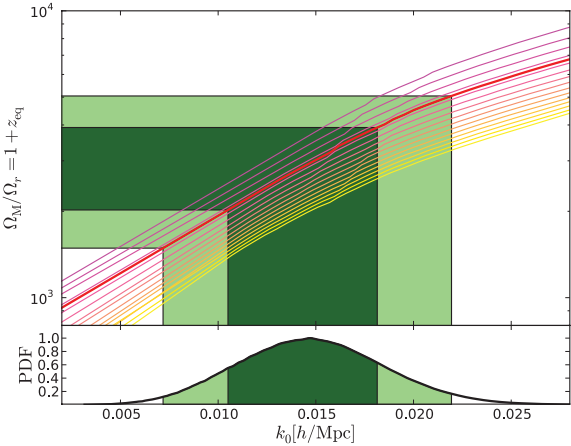


Figure 4. Bottom panel: the 1D marginalized PDF for k_0 from fitting our logarithmic parabola turnover model (see equation 4) to the observed WiggleZ $P(k)$. The dark-shaded regions depict 68 per cent confidence intervals and the light-shaded regions depict 95 per cent confidence intervals. Top panel: an illustration of how our constraint on k_0 maps to a constraint on $\Omega_M/\Omega_r = 1 + z_{\text{eq}}$. The lines depict the dependence of $1 + z_{\text{eq}}$ on k_0 , calibrated using `CAMB`, for several values of N_{eff} (increasing from $N_{\text{eff}} = 0$ in magenta to $N_{\text{eff}} = 10$ in yellow, in steps of 0.67; $\Omega_M h^2$ increases from the left-hand to right-hand side). We highlight the relation for $N_{\text{eff}} = 3$ in red as well as the constraint on $1 + z_{\text{eq}}$ determined from our measurement of k_0 for this case.

the dependence of the redshift of matter–radiation equality on Ω_M and Ω_r given by

$$1 + z_{\text{eq}} = \frac{\Omega_M}{\Omega_r} = \frac{\Omega_M h^2}{\Omega_\gamma h^2} \frac{1}{1 + 0.2271 N_{\text{eff}}}. \quad (11)$$

From this we can convert our constraints on the turnover scale into constraints on $\Omega_M h^2$, N_{eff} and subsequently z_{eq} as follows. In Fig. 4 we plot the ratio Ω_M/Ω_r as a function of the turnover scale (k_0) measured from our `CAMB` power spectra for a range of N_{eff} between 0 and 10. Each line represents results for a wide range of values for $\Omega_M h^2$, which increases with increasing k_0 . Projecting an observed turnover scale on to this sequence of curves allows us to map any value of k_0 to a unique set of values for $\Omega_M h^2$ and $\Omega_M/\Omega_r = 1 + z_{\text{eq}}$ as a function of N_{eff} .

To see the form of the resulting constraint in the $N_{\text{eff}} - \Omega_M h^2$ plane, we can rearrange equation (11) to get

$$N_{\text{eff}} = 4.403 \left[\left(\frac{\Omega_M}{\Omega_r} \right)^{-1} (\Omega_\gamma h^2)^{-1} (\Omega_M h^2) - 1 \right], \quad (12)$$

where the first bracketed factor is constrained from the turnover measurement and the second bracketed factor is known precisely from the CMB. Hence, we expect the scale of the turnover to place a roughly linear degenerate constraint in this plane, since our one measurement cannot place closed constraints on two values.

We also show in Fig. 5 the *WMAP* CMB constraint in the $N_{\text{eff}} - \Omega_M h^2$ plane. We made use of the $\Lambda\text{CDM} + N_{\text{eff}}$ *WMAP* 7-year chains, downloaded from the *WMAP* LAMBDA data products site,² and analysed them using the `GetDist` package that comes as part of `CosmoMC` (Lewis & Bridle 2002).

Immediately obvious from this plot is the degeneracy in the WiggleZ constraints expressed by equation (12). The *WMAP* constraints also exhibit a strong degeneracy, although oriented

² <http://lambda.gsfc.nasa.gov/product/map/current/>

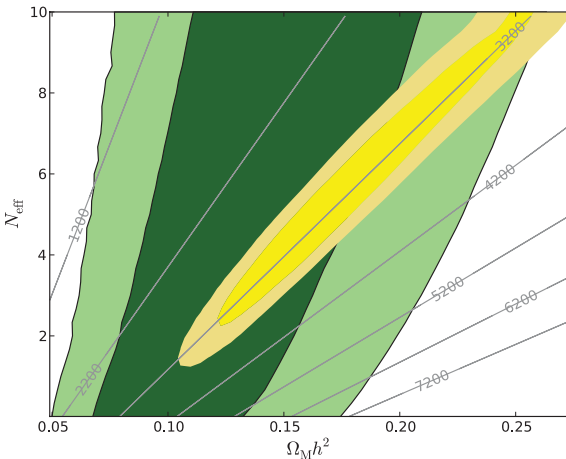


Figure 5. The constraints in the N_{eff} – $\Omega_M h^2$ plane derived from the WiggleZ measurement of the turnover scale (in green) compared to CMB COSMOMC constraints from *WMAP* (in yellow). The dark-shaded regions depict 68 per cent confidence intervals and the light-shaded regions depict 95 per cent confidence intervals. The grey contours depict lines of constant $\Omega_M/\Omega_r = 1 + z_{\text{eq}}$.

differently and along the line $1 + z_{\text{eq}} \sim 3200$. While this degeneracy does not close for the WiggleZ constraint, it does for the *WMAP* constraint, demanding $N_{\text{eff}} \gtrsim 2$. While we do not perform a rigorous joint fit of these measurements, it is clear that the WiggleZ turnover constraint should help to close the CMB constraints at an upper limit $N_{\text{eff}} \lesssim 9$.

While our measurement of the WiggleZ turnover scale clearly provides little constraint on N_{eff} (even with a strong prior on $\Omega_M h^2$), a constraint on $\Omega_M h^2$ can be derived, given a prior on N_{eff} . Assuming the value $N_{\text{eff}} = 3$, we obtain a WiggleZ turnover constraint of $\Omega_M h^2 = 0.136^{+0.026}_{-0.052}$ (68 per cent) and $0.136^{+0.073}_{-0.074}$ (95 per cent). As illustrated by equation (11), given a strong prior on N_{eff} , the fractional constraint on $\Omega_M h^2$ maps almost identically to a fractional constraint on z_{eq} . Thus, we find that the WiggleZ turnover provides the constraint $z_{\text{eq}} = 3274^{+631}_{-1259}$ (68 per cent) and 3274^{+1757}_{-1791} (95 per cent). All results are unchanged if the expected value $N_{\text{eff}} = 3.046$ is taken for the assumed prior instead.

4 FORECASTS FOR FUTURE SURVEYS

From these results, the question naturally arises: what sort of constraint on N_{eff} , $\Omega_M h^2$ and z_{eq} would be possible from a larger survey such as BOSS or *Euclid*, encompassing a larger volume and hence providing a stronger turnover constraint?

In this section, we examine the prospects of using the turnover position in current and future surveys for cosmology constraints. The key questions we seek to answer are: how effective will turnover constraints on N_{eff} and $\Omega_M h^2$ be from BOSS and *Euclid* and how big

does a survey need to be for these constraints to be competitive with those from CMB observations? The results of these calculations are summarized and compared to our WiggleZ measurements in Table 2.

We will find that the required volumes are large but it is important to note that photometric redshift surveys for which imaging systematics are under good control are just as effective for this science as spectroscopic redshift surveys. This is because the distance uncertainties associated with photometric redshift errors will be small compared to the scales of the turnover (Blake & Bridle 2005).

4.1 Constructing mock survey constraints

We have repeated the analysis presented in Section 3 on a series of mock power spectra generated using CAMB in our fiducial cosmology and given ranges in k and noise properties designed to represent future surveys. We ignore the complicating issues of survey selection and geometry and assume that the scales relevant to this analysis remain volume limited in their precision. Under these conditions, survey volume (denoted by V) is the only survey parameter relevant to our calculation. In all cases, we assume that the largest scale probed is $L_{\text{max}} = \sqrt[3]{V}$ and choose a power spectrum binning given by $\Delta k = 2\pi/L_{\text{max}}$. In each case, we combine 20 chains for the analysis of each forecast survey volume, each with differing random seeds for the noise generation process.

For these calculations, we have changed the maximum value of k over which we perform our turnover fits to $k_{\text{max}} = 0.04$ ($h \text{ Mpc}^{-1}$). This was done to avoid a systematic bias introduced by the BAO features of the power spectrum which becomes significant when volumes exceed those of WiggleZ. This bias is driven by a degeneracy between β and k_0 and a dependence of β on k_{max} .

We also slightly change the functional form of our model power spectrum for this calculation. With a sufficiently large volume, the primordial power spectrum should begin to emerge in a survey's largest modes. The primordial power spectrum is expected to be a power law (or nearly so), which differs substantially from the simple asymmetric logarithmic parabola model of equation (4). To capture this behaviour in our forecasts for surveys with very large volumes, we instead use for our power spectrum model an asymmetric logarithmic hyperbola on scales larger than the turnover. Equation (1) then becomes

$$\log_{10} P(k) = \begin{cases} \log_{10} P_0 + p - \sqrt{\alpha^2 x^2 + p^2} & \text{if } k < k_0, \\ \log_{10} P_0 (1 - \beta x^2) & \text{if } k \geq k_0. \end{cases} \quad (13)$$

This model adds an additional degree of freedom (p) which describes how quickly $P(k)$ asymptotes to a power law at $k < k_0$. We have verified that using this model on the observed WiggleZ $P(k)$ and on model power spectra of comparable volume generates consistent results for the turnover scale.

Table 2. A summary of our WiggleZ turnover-derived cosmology measurements and of our forecasts for the precisions of turnover-derived and CMB results in future/ongoing surveys. The unbracketed quantities are 68 per cent confidence results and bracketed quantities are 95 per cent confidence results.

Survey	k_0	$\Omega_M h^2$	z_{eq}	N_{eff}
WiggleZ measurement	$0.0160^{+0.0035}_{-0.0041}$	$(^{+0.0073}_{-0.0075})$	$0.136^{+0.026}_{-0.052}$	$(^{+0.073}_{-0.074})$
BOSS forecast precision	± 9 per cent	$(\pm 16$ per cent)	± 10 per cent	$(\pm 20$ per cent)
<i>Euclid</i> forecast precision	± 3 per cent	$(\pm 5$ per cent)	± 4 per cent	$(\pm 6$ per cent)
<i>Planck</i> forecast precision	–	–	± 3 per cent	$(\pm 5$ per cent)
				± 2 per cent
				$(\pm 4$ per cent)
				± 9 per cent
				$(\pm 14$ per cent)

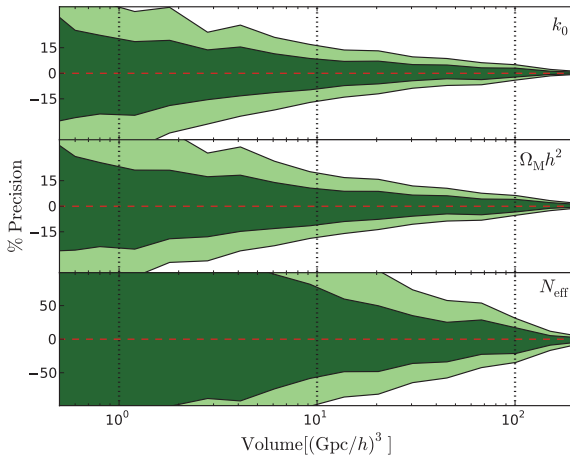


Figure 6. The precision of turnover scale (k_0) measurements and subsequent constraints on $\Omega_M h^2$ and N_{eff} as a function of survey volume. The vertical dotted lines indicate the approximate volume of WiggleZ, BOSS and *Euclid* in order of increasing volume. For the $\Omega_M h^2$ constraints an $N_{\text{eff}} = 3$ prior is assumed and for the N_{eff} constraints an $\Omega_M h^2 = 0.135$ prior is assumed (although results are insensitive to these choices). The dark-shaded regions depict 68 per cent confidence intervals and the light-shaded regions depict 95 per cent confidence intervals.

4.2 Forecast results

The results of our survey forecasts are shown in Fig. 6 where we present, as a function of survey volume, the precision of the turnover scale measurement and of the resulting constraints on $\Omega_M h^2$ and N_{eff} . For the $\Omega_M h^2$ constraints, an $N_{\text{eff}} = 3$ prior is assumed and for the N_{eff} constraints, an $\Omega_M h^2 = 0.135$ prior is assumed. Results are insensitive to these choices however, particularly for large volumes.

In this figure, we highlight the results for survey volumes approximately equal to those of WiggleZ, BOSS and *Euclid* representing a series covering the range of our calculations in logarithmically equal steps in volume. BOSS (Eisenstein et al. 2011) will map $10\,000 \text{ deg}^2$, collecting spectroscopic redshifts for LRGs out to $z \sim 0.7$. With the completion planned for 2014, BOSS represents the largest survey for which near-term results will be possible. The *Euclid* satellite (Laureijs et al. 2011) will conduct a wide-field ($15\,000 \text{ deg}^2$) extragalactic survey covering redshifts out to $z \sim 2$. With a target launch date in 2017–2018, the anticipated specifications of this survey represent a rough limit to our capabilities for conducting the science discussed here at the turn of the next decade.

In Fig. 6 we see that results for $V \sim 1 (\text{Gpc } h^{-1})^3$ are roughly consistent with the WiggleZ constraints (although slightly better, presumably due to the lack of covariance in our forecast model) presented in Figs 3–5: a k_0 precision of ± 20 per cent (68 per cent) and ± 40 per cent (95 per cent) with little resulting constraint on $N_{\text{eff}} \lesssim 10$. The 24 per cent precision of the constraint on $\Omega_M h^2$ (and thus, z_{eq}) for this case maps almost directly to the precision of the constraint on k_0 .

As the volume approaches that of BOSS at $V \sim 10 (\text{Gpc } h^{-1})^3$, the nature of these constraints changes significantly. With a sizeable increase in the number and accuracy of measured modes and scales beyond the turnover, the constraints on k_0 improve dramatically to a precision of ± 9 per cent (68 per cent) and ± 16 per cent (95 per cent). This translates to significantly improved constraints on $\Omega_M h^2$ and z_{eq} of ± 10 per cent (68 per cent) and ± 20 per cent (95 per cent). The constraints on N_{eff} start to become interesting at a level of $^{+78}_{-56}$ per cent (68 per cent) and $^{+152}_{-98}$ per cent (95 per cent) as well.

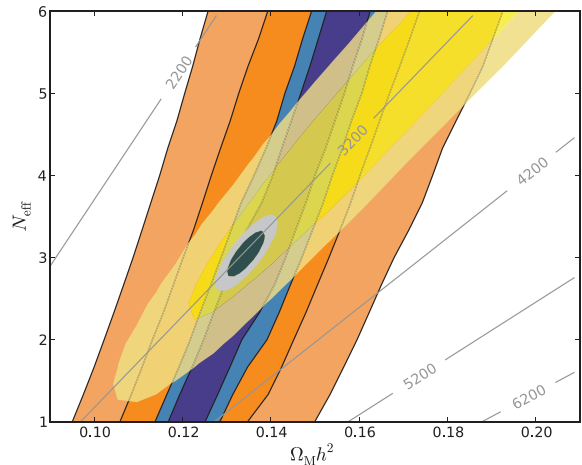


Figure 7. The constraints in the $N_{\text{eff}}-\Omega_M h^2$ plane derived from our forecasts for the BOSS (in orange) and *Euclid* (in blue) measurements of the turnover scale. These are compared to the CMB constraint from *WMAP* (in yellow) and our *Planck* forecast (in grey). The dark-shaded regions depict 68 per cent confidence intervals and the light-shaded regions depict 95 per cent confidence intervals. The grey contours depict lines of constant $\Omega_M/\Omega_r = 1 + z_{\text{eq}}$.

Looking past BOSS to much larger future surveys, the precision improves more slowly with increasing volume. However, with $V \sim 100 (\text{Gpc } h^{-1})^3$, the proposed volume of *Euclid*³ is a dramatic order-of-magnitude increase over BOSS. As a result, *Euclid* should ultimately be able to measure k_0 to a precision of ± 3 per cent (68 per cent) and ± 5 per cent (95 per cent) with corresponding constraints on $\Omega_M h^2$ and z_{eq} of ± 4 per cent (68 per cent) and ± 6 per cent (95 per cent) and on N_{eff} of $^{+17}_{-21}$ per cent (68 per cent) and $^{+32}_{-35}$ per cent (95 per cent).

We contrast these forecasts with the results anticipated from *Planck*. For our *Planck* constraints we generated simulated *Planck* data following the procedure used in Perotto et al. (2006) using the specifications for the HFI bolometers given in the Planck Blue Book (The Planck Collaboration 2006). We then used *COSMOMC* to generate chains, assuming a $\Lambda\text{CDM}+N_{\text{eff}}$ model.

In Fig. 7 we illustrate our forecast constraints for BOSS and *Euclid* in the $N_{\text{eff}}-\Omega_M h^2$ plane, compared to the CMB constraints of *WMAP* and our forecasts for the *Planck Surveyor*. We can see from this figure that BOSS should make important contributions to the present *WMAP* constraint, closing the upper limit of the 68 per cent confidence contours at $N_{\text{eff}} \lesssim 6$. Looking to the future however, we see the dramatic improvement *Planck* will make to this measurement. In detail, we find the constraints from *Planck* on $(\Omega_M h^2, N_{\text{eff}}, z_{\text{eq}})$ should be $\pm 3, \pm 9$ and ± 2 per cent (68 per cent confidence) and $\pm 5, \pm 14$ and ± 4 per cent (95 per cent confidence), respectively. While this constraint on z_{eq} is significantly better than what *Euclid* will provide on its own (even with strong priors), the constraints on $\Omega_M h^2$ and N_{eff} are otherwise comparable.

5 SUMMARY AND CONCLUSIONS

We have presented an analysis of the WiggleZ Dark Energy Survey, constructing a galaxy power spectrum optimized for studying the largest scales of the survey. We extract from this the most robust

³ From the Euclid Science Requirements Document, ESA Science document reference number DEM-SA-Dc-00001.

measurement to date of the scale of the turnover in the Universe's matter power spectrum. From this, we have obtained the first distance measurement and cosmology constraints yet derived from measurements of this feature. We have also constructed forecasts for the precision of this analysis for future surveys, contrasting the constraints we expect to obtain from turnover measurements in future redshift surveys to complementary constraints from the published observations of *WMAP* and our forecasts for the *Planck Surveyor*.

Details of our results from the analysis of the WiggleZ data set (all uncertainties quoted at 68 per cent confidence) are as follows:

(i) We present an MCMC method which removes window function convolution effects while co-adding the individual observed power spectra of a galaxy survey observed over several disconnected regions.

(ii) Applying this method to WiggleZ data we find that the survey is able to probe modes at and beyond the scale of the turnover.

(iii) Using an MCMC approach, we have fitted an asymmetric logarithmic parabola to the observed WiggleZ power spectrum. From this analysis, we find the scale of the turnover to be $k_0 = 0.0160^{+0.0035}_{-0.0041}$. This is in excellent agreement with our fiducial standard Λ CDM value of $k_0 = 0.016$ (Mpc h^{-1}).

(iv) Parametrizing the power spectrum beyond the scale of the turnover as $P(k < k_0) \propto k^n$, we find $n > -1$ at nearly 95 per cent confidence. The standard Λ CDM value of $n = 1$ is easily accommodated by our fit.

(v) The continuance at large scales of the small-scale asymptotic value of $n = -3$ is completely ruled out by our analysis.

(vi) We have performed the first measurement of the peak position in the cosmological power spectrum, representing the first secure and quantified observation of this feature to date.

From this measurement, we then extract – for the first time using a measurement of the turnover scale – the following information:

(i) A model-independent distance measurement to $z = 0.62$ in units of the $z = 3145$ horizon scale at the redshift of matter–radiation equality (r_H) of $D_V(z_{\text{eff}} = 0.62)/r_H = 18.3^{+6.3}_{-3.3}$

(ii) A measurement of the cosmological density parameter $\Omega_M h^2 = 0.136^{+0.026}_{-0.052}$ (assuming an $N_{\text{eff}} = 3$ prior)

(iii) A measurement of the redshift of matter–radiation equality $z_{\text{eq}} = 3274^{+631}_{-1260}$ (assuming an $N_{\text{eff}} = 3$ prior).

Looking to the future, we have computed forecasts for the turnover precision attainable by BOSS and *Euclid*. We find that BOSS should substantially improve upon the results presented here, reaching precisions in $(k_0, \Omega_M h^2, z_{\text{eq}}, N_{\text{eff}})$ of $(\pm 9, \pm 10, \pm 10, \pm 78)$ per cent, respectively. This represents sufficient precision to sharpen the constraints on N_{eff} from *WMAP*, particularly in its upper limit. For *Euclid*, we find corresponding attainable precisions of $(\pm 3, \pm 4, \pm 4, \pm 17)$ per cent. This represents a precision approaching our forecasts for *Planck*.

We emphasize that these results are all obtained within the theoretical framework of Gaussian primordial fluctuations. In the event that cosmological structure formation was seeded by non-Gaussian fluctuations, scale-dependent bias effects may substantially change the standard Λ CDM predictions for $P(k)$ on scales comparable to and larger than the turnover (Dalal et al. 2008; Desjacques, Seljak & Iliev 2009; Giannantonio & Porciani 2010; Desjacques, Jeong & Schmidt 2011a,b). Measurements of primordial Gaussianity from studies of large-scale structure have proven to provide constraints of comparable precision to those from the CMB (Slosar et al. 2008) with forecasts for future surveys suggesting that the two approaches

will remain complementary for some time (Giannantonio et al. 2012). Interestingly, current constraints allow for cases where the power spectrum exhibits no turnover but merely an inflection at turnover scales, with $P(k)$ being a declining function of k at large scales. Many such models are compatible with the results presented in this study but the lower limit we place on n in the large-scale limit of $P(k) \propto k^n$ suggests that the WiggleZ power spectrum measurement may be capable of constraining their allowed parameter ranges. However, such effects are expected to scale with galaxy bias b as $(b-1)$ (e.g. Dalal et al. 2008) and WiggleZ galaxies are known to have a bias near unity (e.g. Blake et al. 2010), greatly reducing the degree of such effects for this survey. Regardless, we forgo this analysis for now and focus instead on the case of purely Gaussian primordial fluctuations. Future studies involving WiggleZ bispectrum measurements will address this science.

Furthermore, while this paper focuses on the scale of the turnover as a cosmological constraint, there is much more information present in the full shape of the power spectrum which could provide (for example) constraints on $\Omega_M h^2$ (see Parkinson et al. 2012), tightening the constraints presented here not only on this parameter but also on N_{eff} . Such a situation is similar to that of BAO studies where final cosmological constraints tend to incorporate information from both the BAO scale and the shape of the underlying power spectrum (see e.g. fig. 6 of Blake et al. 2011c). As such, the constraints presented here likely represent underestimates of the true potential of these experiments.

Finally, with increased constraints on N_{eff} and $\Omega_M h^2$, the absolute scale of the turnover could be accurately calibrated, permitting its use as a standard ruler for measuring the distance–redshift relation. Our forecasts suggest that a regular volume of $V \sim 10$ (Gpc h^{-1})³ with a well-defined effective redshift would permit a distance measurement of roughly 10 per cent accuracy. *Euclid*, for instance, could provide several such volumes arranged across redshift, perhaps enabling the first measurement of a Hubble diagram using the turnover scale as a standard ruler. Given the purely linear evolution of the matter power spectrum on scales of the turnover, this could provide a powerful check against systematic redshift-dependent biases in BAO studies.

ACKNOWLEDGMENTS

We thank Francesco Montesano for his constructive and insightful examination of our manuscript. We acknowledge financial support from the Australian Research Council through Discovery Project grants DP0772084 and DP1093738 and Linkage International travel grant LX0881951. GBP thanks Simon Mutch for his help with developing the MCMC code used for the analysis in this study. CB acknowledges the support of the Australian Research Council through the award of a Future Fellowship. SC and DJC acknowledge the support of Australian Research Council QEII Fellowships. MJD and TD thank the Gregg Thompson Dark Energy Travel Fund for financial support. The *Galaxy Evolution Explorer* (GALEX) is a NASA Small Explorer, launched in 2003 April. We gratefully acknowledge NASA's support for construction, operation and science analysis for the GALEX mission, developed in cooperation with the Centre National d'Etudes Spatiales of France and the Korean Ministry of Science and Technology. We thank the Anglo-Australian Telescope Allocation Committee for supporting the WiggleZ survey over nine semesters, and we are very grateful for the dedicated work of the staff of the Australian Astronomical Observatory in the development and support of the AAOmega spectrograph, and the running of the Anglo-Australian Telescope. We are also grateful for support

from the Centre for All-sky Astrophysics, an Australian Research Council Centre of Excellence funded by grant CE11000102.

REFERENCES

- Anderson L. et al., 2012, preprint (arXiv:1203.6594)
- Archidiacono M., Calabrese E., Melchiorri A., 2011, Phys. Rev. D, 84, 123008
- Baugh C. M., Efstathiou G., 1993, MNRAS, 265, 145
- Baugh C. M., Efstathiou G., 1994, MNRAS, 267, 323
- Beutler F. et al., 2011, MNRAS, 416, 3017
- Blake C., Bridle S., 2005, MNRAS, 363, 1329
- Blake C. et al., 2010, MNRAS, 406, 803
- Blake C. et al., 2011a, MNRAS, 418, 1707
- Blake C. et al., 2011b, MNRAS, 415, 2876
- Blake C. et al., 2011c, MNRAS, 415, 2892
- Calabrese E., Archidiacono M., Melchiorri A., Ratra B., 2012, Phys. Rev. D, 86, 043520
- Cole S. et al., 2005, MNRAS, 362, 505
- The Planck Collaboration, 2006, preprint (arXiv:astro-ph/0604069)
- Dalal N., Doré O., Huterer D., Shirokov A., 2008, Phys. Rev. D, 77, 123514
- Desjacques V., Seljak U., Iliev I. T., 2009, MNRAS, 396, 85
- Desjacques V., Jeong D., Schmidt F., 2011a, Phys. Rev. D, 84, 61301
- Desjacques V., Jeong D., Schmidt F., 2011b, Phys. Rev. D, 84, 63512
- Drinkwater M. J. et al., 2010, MNRAS, 401, 1429
- Dunkley J. et al., 2011, ApJ, 739, 52
- Durrer R., Gabrielli A., Joyce M., Labini F. S., 2003, ApJ, 585, L1
- Einasto J., Gramann M., Saar E., Tago E., 1993, MNRAS, 260, 705
- Einasto J., Einasto M., Tago E., Starobinsky A. A., Atrio-Barandela F., Müller V., Knebe A., Cen R., 1999, ApJ, 519, 469
- Eisenstein D. J., Hu W., 1998, ApJ, 496, 605
- Eisenstein D. J. et al., 2005, ApJ, 633, 560
- Eisenstein D. J. et al., 2011, AJ, 142, 72
- Feldman H. A., Kaiser N., Peacock J. A., 1994, ApJ, 426, 23 (FKP)
- Fixsen D. J., 2009, ApJ, 707, 916
- Giannantonio T., Porciani C., 2010, Phys. Rev. D, 81, 63530
- Giannantonio T., Porciani C., Carron J., Amara A., Pillepich A., 2012, MNRAS, 422, 2854
- Hou Z., Keisler R., Knox L., Millea M., Reichardt C., 2011, preprint (arXiv:1104.2333)
- Jing Y. P., 2005, ApJ, 620, 559
- Kaiser N., 1987, MNRAS, 227, 1
- Keisler R. et al., 2011, ApJ, 743, 28
- Komatsu E. et al., 2009, ApJS, 180, 330
- Komatsu E. et al., 2011, ApJS, 192, 18
- Laureijs R. et al., 2011, preprint (arXiv:1110.3193)
- Lewis A., Bridle S., 2002, Phys. Rev. D, 66, 103511
- Lewis A., Challinor A., Lasenby A., 2000, ApJ, 538, 473
- Li I. H. et al., 2012, ApJ, 747, 91
- Mangano G., Miele G., Pastor S., Pinto T., Pisanti O., Serpico P. D., 2005, Nucl. Phys. B, 729, 221
- Outram P. J., Hoyle F., Shanks T., Croom S. M., Boyle B. J., Miller L., Smith R. J., Myers A. D., 2003, MNRAS, 342, 483
- Padmanabhan N. et al., 2007, MNRAS, 378, 852
- Parkinson D. et al., 2012, Phys. Rev. D, 86, 103518
- Peacock J. A., Nicholson D., 1991, MNRAS, 253, 307
- Peacock J. A., West M. J., 1992, MNRAS, 259, 494
- Perotto L., Lesgourgues J., Hannestad S., Tu H., Wong Y. Y. Y., 2006, J. Cosmol. Astropart. Phys., 10, 013
- Prada F., Klypin A., Yepes G., Nuza S. E., Gottloeber S., 2011, preprint (arXiv:1111.2889)
- Riemer-Sørensen S. et al., 2012, Phys. Rev. D, 85, 81101
- Ross A. J. et al., 2011, MNRAS, 417, 1350
- Ross A. J. et al., 2012, MNRAS, 424, 564
- Scaramella R., 1993, MNRAS, 262, L43
- Slosar A., Hirata C., Seljak U., Ho S., Padmanabhan N., 2008, J. Cosmol. Astropart. Phys., 08, 031
- Smith R. E. et al., 2003, MNRAS, 341, 1311
- Smith T. L., Das S., Zahn O., 2012, Phys. Rev. D, 85, 23001
- Tadros H., Efstathiou G., Dalton G., 1998, MNRAS, 296, 995
- Wisnioski E. et al., 2011, MNRAS, 417, 2601
- Yoo J., 2010, Phys. Rev. D, 82, 83508
- York D. G. et al., 2000, AJ, 120, 1579

This paper has been typeset from a $\text{\TeX}/\text{\LaTeX}$ file prepared by the author.